TOXICOLOGICAL SCIENCES, 163(2), 2018, 543–556

doi: 10.1093/toxsci/kfy060
Advance Access Publication Date: March 27, 2018
Research Article

Metabolic Activation of the Cooked Meat Carcinogen 2-Amino-1-Methyl-6-Phenylimidazo[4,5-*b*]Pyridine in Human Prostate

Medjda Bellamri,* Shun Xiao,* Paari Murugan,† Christopher J. Weight,‡ and Robert J. Turesky*,[1]

*Masonic Cancer Center and Department of Medicinal Chemistry, Cancer and Cardiovascular Research Building; †Department of Laboratory Medicine and Pathology; and ‡Department of Urology, University of Minnesota, Minneapolis, Minnesota 55455

[1]To whom correspondence should be addressed at Masonic Cancer Center and Department of Medicinal Chemistry, Cancer and Cardiovascular Research Building, University of Minnesota, 2231 6th Street, Minneapolis, MN 55455. E-mail: rturesky@umn.edu.

The authors certify that all research involving human subjects was done under full compliance with all government policies and the Helsinki Declaration.

ABSTRACT

2-Amino-1-methyl-6-phenylimidazo[4,5-*b*]pyridine (PhIP), an heterocyclic aromatic amine (HAA) formed in cooked meat, is a rodent and possible human prostate carcinogen. Recently, we identified DNA adducts of PhIP in the genome of prostate cancer patients, but adducts of 2-amino-3, 8-dimethylmidazo[4,5-*f*]quinoxaline (MeIQx) and 2-amino-9*H*-pyrido[2,3-*b*]indole (AαC), other prominent HAAs formed in cooked meats, were not detected. We have investigated the bioactivation of HAAs by Phase I and II enzymes in the human prostate (LNCaP) cell line using cytotoxicity and DNA adducts as endpoints. PhIP, MeIQx, and 2-amino-3-methylimidazo[4,5-*f*]quinoline, another HAA found in cooked meats, were poorly bioactivated and not toxic. The synthetic genotoxic N-hydroxylated-HAAs were also assayed in LNCaP cells with Phase II enzyme inhibitors. Notably, 2-hydroxy-amino-1-methyl-6-phenylimidazo[4,5-*b*]pyridine (HONH-PhIP), but not other HONH-HAAs, induced cytotoxicity. Moreover, PhIP-DNA adduct formation was 20-fold greater than adducts formed with other HONH-HAAs. Pretreatment of LNCaP cells with mefenamic acid, a specific inhibitor of sulfotransferase (SULT1A1), decreased PhIP-DNA adducts by 25%, whereas (*Z*)-5-(2′-hydroxybenzylidene)-2-thioxothiazolidin-4-one and pentachlorophenol, inhibitors of SULTs and N-acetyltransferases (NATs), decreased the PhIP-DNA adduct levels by 75%. NATs in cytosolic fractions of LNCaP cells and human prostate catalyzed DNA binding of HONH-PhIP by up to 100-fold greater levels than for SULT and kinase activities. Recombinant NAT2 is catalytically superior to recombinant NAT1 in the bioactivation of HONH-PhIP; however, the extremely low levels of NAT2 activity in prostate suggest that NAT1 may be the major isoform involved in PhIP-DNA damage. Thus, the high susceptibility of LNCaP cells recapitulates the DNA-damaging effect of HONH-PhIP in rodent and human prostate.

Key words: prostate cancer; heterocyclic aromatic amines; 2-amino-1-methyl-6-phenylimidazo[4,5-*b*]pyridine; DNA adduct; metabolic activation.

Prostate cancer (PC) is the most commonly diagnosed noncutaneous cancer in men and the second leading cause of cancer-related death in men (Siegel *et al.*, 2016). The major risk factors for PC are increasing age, family history, and African American ethnicity (Bostwick *et al.*, 2004). PC is most prevalent in affluent countries (McGuire, 2016). Epidemiological studies have reported large geographical variations in incidence and mortality of PC and that lifestyle factors influence the risk of PC

(Gann, 2002). Dairy products, red meats, and a high-fat diet are risk factors for PC (Mandair *et al.*, 2014). Red meat is classified, by the International Agency for Research on Cancer (IARC), as probably carcinogenic to humans (Group 2 A), with an increased risk of colorectal cancer but also elevated risks of pancreatic cancer and PC (Bouvard *et al.*, 2015).

More than 25 heterocyclic aromatic amines (HAAs) are formed in cooked red meats (Felton *et al.*, 2000; Sugimura *et al.*, 2004; Turesky and Le Marchand, 2011). HAAs are multisite carcinogens in rodents (Sugimura *et al.*, 2004). 2-Amino-1-methyl-6-phenylimidazo[4,5-*b*]pyridine (PhIP) is an abundant carcinogenic HAA formed in well-done cooked red meats (Knize and Felton, 2005). PhIP and other HAAs are classified as possible human carcinogens (Group 2 A or 2B) by IARC (IARC, 1993). PhIP, in contrast to other HAAs, targets the prostate as a major site of DNA adduct formation and genotoxicity in rodents (Sugimura *et al.*, 2004). PhIP increases the mutation frequency of the *lacI* transgene in the prostate of transgenic big blue rats (Stuart *et al.*, 2000) and induces prostate tumors in CYP1A-humanized (hCYP1A) mice (Li *et al.*, 2012) and in Fischer 344 rats (Shirai *et al.*, 1997), whereas other HAAs do not induce PC (Sugimura *et al.*, 2004). In hCYP1A-mice, PhIP induces inflammation, epithelial cell damage, and prostatic intraepithelial neoplasia in the dorsolateral prostate lobe compared to the ventral lobe (Li *et al.*, 2012). These observations are significant, since the dorsolateral prostate lobe is homologous to the peripheral zone of the human prostate, where up to 80% of prostate adenocarcinoma occurs (Oliveira *et al.*, 2016). PhIP forms DNA adducts in the prostate, but it also induces oxidative stress, atrophy of the acini, and inflammation of the prostate of rodents (Borowsky *et al.*, 2006; Nakai *et al.*, 2007; Shirai, *et al.*, 1997). These features are observed in the pathology of human PC (Nakai and Nonomura, 2013).

HAAs require metabolic activation to exert their genotoxic effects (Turesky and Le Marchand, 2011). The metabolism of HAAs occurs in the liver, but the extent of HAA metabolism in extrahepatic tissues is not well known. N-Oxidation of the exocyclic amine group is the first step in the bioactivation of HAAs. The formation of 2-hydroxyamino-1-methyl-6-phenylimidazo[4,5-*b*]pyridine (HONH-PhIP) and other HONH-HAAs is catalyzed by CYP1A2 in the liver and by CYP1A1 and CYP1B1 in extrahepatic tissues (Turesky and Le Marchand, 2011). Conjugation enzymes, such as N-acetyltransferases (NATs) or sulfotransferases (SULTs), catalyze the conversion of HONH-HAAs to reactive conjugates that undergo heterolytic cleavage to form their presumed short-lived nitrenium ions that covalently adduct to DNA (Turesky and Le Marchand, 2011). The major DNA adduct of PhIP formed in rodents is *N*-(2′-deoxyguanosin-8-yl)-PhIP (dG-C8-PhIP) (Goodenough *et al.*, 2007).

We recently identified dG-C8-PhIP, by liquid chromatography-mass spectrometry (LC-MS), in biopsy samples of PC patients, but we did not detect DNA adducts of other prominent HAAs formed in cooked meats, including 2-amino-9 *H*-pyrido[2,3-*b*]indole (AαC) and 2-amino-3,8-dimethylimidazo[4,5-*f*]quinoxaline (MeIQx) (Xiao *et al.*, 2016). In this study, we investigated the cytotoxicity and DNA binding potential of PhIP compared to AαC, MeIQx, and 2-amino-3-methylimidazo[4,5-*f*]quinoline (IQ), another prototypical HAA formed in cooked meat (Sugimura, *et al.*, 2004), in LNCaP cells, a well-characterized human prostate cell line that maintains a differentiated phenotype (Crow *et al.*, 2005). Our findings show that the parent HAAs are poorly bioactivated by CYPs in LNCaP cells and not cytotoxic under the dose concentrations studied (0.1–10 μM). In contrast, LNCaP cells are highly susceptible to the cytotoxicity of HONH-PhIP but not to the other

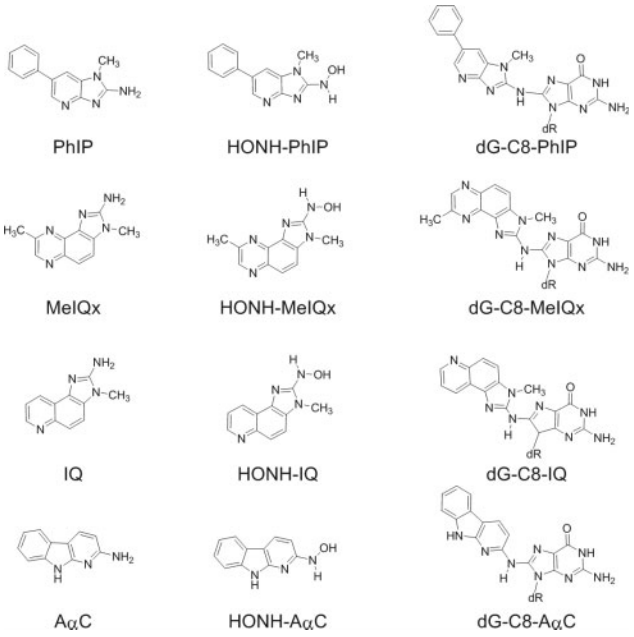

Scheme 1. Chemical structures of HAAs, HONH-HAAs and their DNA adducts.

HONH-HAAs. Moreover, the level of PhIP-DNA binding in LNCaP cells treated with HONH-PhIP is 20-fold or higher than the levels of DNA adducts formed with other HONH-HAAs (Scheme 1). Our studies conducted with inhibitors of Phase II enzymes in LNCaP cells, and LNCaP and human prostate cytosolic fractions reveal an important role for NATs and lesser roles for SULTs and kinases in the bioactivation of HONH-PhIP. The biochemical data obtained with LNCaP cells are consistent with our DNA adduct biomarker data in humans, showing that PhIP is a principal HAA formed in cooked meats that induces DNA damage of the prostate.

MATERIALS AND METHODS

Caution. HAAs are potential human carcinogens and should be handled carefully in well-ventilated hoods and wearing protective clothing.

Chemicals. PhIP, MeIQx, IQ, and AαC were purchased from Toronto-Research Chemicals, Inc (Toronto, Ontario, Canada). Dimethyl sulfoxide (DMSO), pentachlorophenol (PCP), mefenamic acid, (Z)-5-(2′-hydroxybenzylidene)-2-thioxothiazolidin-4-one (Rhod-o-hp), 4-aminobenzoic acid (PABA), N-acetyl-PABA, sulfamethazine (SMZ), N-acetyl-SMZ, 4-nitrophenol, 4-nitrophenylsulfate, β-estradiol, β-estradiol-3-glucuronide, propofol, propofol glucuronide, ethylenediaminetetraacetic acid (EDTA), β-mercaptoethanol (BME), dithiothreitol (DTT), phenylmethanesulfonyl fluoride (PMSF), leupeptin, calf thymus DNA (CT-DNA), adenosine 5-triphosphate (ATP), acetyl coenzyme A (AcCoA), adenosine 3-phosphate 5-phosphosulfate (PAPS), RNase A (bovine pancreas), RNase T1 (*Aspergillus oryzae*), proteinase K (*Tritirachium album*), sodium dodecyl sulfate (SDS), DNase I (type IV, bovine pancreas), alkaline phosphatase (*Escherichia coli*), and nuclease P1 (*Penicillium citrinum*) were purchased from Sigma Aldrich (St Louis, Missouri). Phosphodiesterase I (*Crotalus adamanteus venom*) was purchased from Worthington Biochemical Corp. (Newark, New Jersey). Recombinant human NAT1 and

NAT2 were purchased from Corning (New York). Deidentified human liver tissue samples were from the Tennessee Donor Services, Nashville, TN, and kindly provided by Dr F.P. Guengerich, Vanderbilt University.

Synthesis of HONH-HAAs, N-acetoxy-PhIP, and DNA adducts. HONH-HAAs were prepared by the reduction of their nitro derivatives as described previously (Pathak *et al.*, 2015; Turesky *et al.*, 1991). *N*-(acetyloxy)-2-amino-1-methyl-6-phenylimidazo[4,5-*b*]pyridine (N-acetoxy-PhIP) was prepared by the reaction of HONH-PhIP with acetic anhydride as reported previously (Wang *et al.*, 2015). Unlabeled and stable isotopically labeled internal standards of *N*-(2′-deoxyguanosin-8-yl)-2-amino-1-methyl-6-phenylimidazo[4,5-*b*]pyridine (dG-C8-PhIP), [$^{13}C_{10}$]-dG-C8-PhIP, *N*-(2′-deoxyguanosin-8-yl)-2-amino-3, 8-dimethylimidazo[4,5-*f*]-quinoxaline (dG-C8-MeIQx), [$^{2}H_{3}C$]-dG-C8-MeIQx, *N*-(2′-deoxyguanosin-8-yl)-2-amino-3-methylimidazo[4,5-*f*]quinoline (dG-C8-IQ), [$^{13}C_{10}$]-dG-C8-IQ, *N*-(2′-deoxyguanosin-8-yl)-2-amino-9*H*-pyrido[2, 3-*b*]indole (dG-C8-AαC), and [$^{13}C_{10}$]-dG-C8-AαC were synthesized as described (Bessette *et al.*, 2009).

Cell culture and treatment. The human prostate cancer cell line LNCaP was obtained from the American Type Culture Collection (Manassas, Virginia). Cells were cultured in RPMI-1640 medium (ATCC) supplemented with 10% fetal calf serum (Sigma Aldrich), penicillin (100 IU/ml; Gibco, Life Technologies, Carlsbad, California), and streptomycin (100 μg/ml; Gibco) at 37°C in a humidified atmosphere of 5% CO_2 in air. For DNA adduct experiments, cells were seeded in 6-well plates at a cell density of 1.5×10^6 cells/well. At 80–90% confluence, the cells were washed with prewarmed phosphate-buffered saline (PBS) at 37°C, and the media were renewed with fresh media containing HAAs (1 or 10 μM) or HONH-HAAs (0.1 or 1 μM) or DMSO (0.1%) as a solvent control. For Phase II enzyme inhibition experiments, cells were pretreated with PCP, mefenamic acid, Rhod-o-hp, or DMSO (0.1%) for 30 min, and then HONH-PhIP was added to a final concentration of 0.1 μM. After 2, 8, or 24 h of treatment, the cells were washed 3 times with cold PBS before being scraped into 1 ml of cold PBS. After centrifugation at 200 × *g* for 7 min at 4°C, the PBS was removed and the cell pellets were stored at −80°C until further analysis.

Cytotoxicity assay. Cell viability assays were performed using the Cell Titer 96 H Aqueous Cell Proliferation Assay (MTS assay; Promega, Fitchburg, Wisconsin); 15×10^4 cells/well were seeded in 96-well plates and grown to confluence before treatment with various concentrations HAAs or HONH-HAAs (0.1–10 μM) using 0.1% DMSO as the vehicle. After 24 h of treatment, 20 μl/well of MTS reagent was added, and the cells were incubated at 37°C. After 2 h, the absorbance was measured at 490 nm using a plate reader (Synergy H1 plate reader; Biotek, Winooski, Vermont).

Human prostate tissue collection and treatments. The research protocol was reviewed and approved by the Institutional Review Board at University of Minnesota. The study population consisted of men from Minnesota, Wisconsin, South Dakota, North Dakota, and Iowa, who were diagnosed with PC and underwent radical prostatectomy (mean age: 64.2 ± 8.5). All tissues were obtained from patients diagnosed with PC and underwent radical prostatectomy and consented to participate in this research. Hemotoxylin and eosin-stained slides of tissue specimens were reviewed by the study pathologist (P. Murugan) to confirm tissue samples assayed for DNA adducts, and enzyme activities were largely tumor free. Fresh frozen human prostate tissues (20–25 mg of wet weight of tissue) were thawed on ice and homogenized using a blade homogenizer (Pro Scientific, Oxford, Connecticut) in 4 ml TE buffer (50 mM Tris-HCl containing 10 mM EDTA and 10 mM BME, pH 8.0). The homogenates were then centrifuged at 3000 × *g* for 10 min at 4°C, and DNA was isolated from the pellet by the phenol/chloroform extraction method as described previously (Xiao *et al.*, 2016). For LNCaP cells, cell pellets ($1.5–2 \times 10^6$) were homogenized in TE buffer (300 μl, 50 mM Tris-HCl containing 10 mM EDTA and 10 mM BME, pH 8.0), and DNA was extracted using the Gentra Puregene kit (Qiagen, Valencia, California) as described previously (Cai *et al.*, 2017). The DNA was washed with 70% ethanol and reconstituted in LC-MS grade water. The concentration of DNA was determined using an Agilent 8453 UV/vis spectrophotometer (Agilent Technologies, Santa Clara, California).

DNA digestion. Twenty μg of DNA from human prostate tissue was spiked with isotopically labeled internal standards ([$^{13}C_{10}$]-dG-C8-PhIP, [$^{13}C_{10}$]-dG-C8-AαC, [$^{2}H_{3}C$]-dG-C8-MeIQx, each at a level of 3 adducts per 10^8 nucleotides bases) or ∼10 μg of DNA from LNCaP cells containing isotopically labeled internal standards ([$^{13}C_{10}$]-dG-C8-PhIP, [$^{2}H_{3}C$]-dG-C8-MeIQx, [$^{13}C_{10}$]-dG-C8-IQ and [$^{13}C_{10}$]-dG-C8-AαC at 1 adduct per 10^7 bases each) were digested in 5 mM Bis-Tris-HCl buffer (pH 7.1) as described previously (Nauwelaers *et al.*, 2011).

Ultraperformance liquid chromatography-electrospray ionization multistage scan mass spectrometry measurement of DNA adducts. The measurement of DNA adducts formed in LNCaP cells and cytosolic DNA binding experiments was performed by ultraperformance liquid chromatography-electrospray ionization multistage scan mass spectrometry (UPLC-ESI/MS^3) with a NanoAcquity UPLC system (Waters Corp, New Milford, Massachusetts) equipped with a Thermo Acclaim trap column (180 μm × 20 mm, 5 μm particle size), a Michrom Magic C18 AQ column (0.3 mm × 150 mm, 3 μm particle size), and a Michrom Captive Spray source interfaced with a linear quadrupole ion trap mass spectrometer Velos Pro (Thermo Fisher, San Jose, California). The chromatography conditions, MS parameters, and the MS^3 transitions used to monitor the protonated ions of DNA adducts were described previously (Nauwelaers, *et al.*, 2011). External calibration curves were constructed for quantification (Goodenough, *et al.*, 2007). The DNA adducts formed in human prostate biopsies were analyzed by high-resolution accurate mass measurements employing a nano LC-Orbitrap-MS^n with a Dionex UltiMate 3000 RSLCnano UHPLC System equipped with a NanoAcquity 10 K 2 G V/V UPLC Symmetry C18 trap column (180 μm × 20 mm, 5 μm particle size; Waters Corp) interfaced with a Nanospray Flex ion source and an Orbitrap Fusion Tribrid MS (Thermo Fisher Scientific). The DNA adducts were monitored at the MS^2 scan stage, employing the chromatography conditions, the MS parameters, and MS^2 transitions reported previously (Xiao, *et al.*, 2016).

Kinetic studies on the stability and metabolism of HONH-PhIP and HONH-MeIQx in LNCaP cells. LNCaP cells were seeded in 6-well plates at a cell density of 1.5×10^6 cells/well. At 80–90% confluence, the cells were washed with warm PBS, and the media were renewed with phenol red-free media containing HONH-PhIP or HONH-MeIQx (1 μM). After 0, 2, 3, 4, and 6 h of incubation, 300 μl of the cell culture media was collected and mixed with 1 volume of cold acetonitrile. After 10 min of incubation on ice, the mixture was centrifuged at 21 000 × g for 10 min, and

the supernatants were analyzed by high-performance liquid chromatography (HPLC) using an Agilent 1260 Infinity model (Agilent, Palo Alto, CA) equipped with ultraviolet (UV)/visible (vis) detector. An Aquasil C18 column (4.6 × 250 mm, 5 μm particle size) from Thermo Scientific (Bellefonte, Pennsylvania) was used with a linear gradient starting from 99% 10 mM ammonium acetate and 1% acetonitrile and ramped to 100% acetonitrile in 20 min at a flow of 1 ml/min. The absorbance was monitored at 316 nm for PhIP, 274 nm for MeIQx, 320 nm for HONH-PhIP, and 274 nm for HONH-MeIQx.

Phase II enzyme activities. The activities of all Phase II enzymes were determined in intact LNCaP cells. The cells were seeded in 6-well plates at a cell density of 1.5×10^6 cells/well. Once 80–90% confluence was reached, the cells were washed with warm PBS, and the cells culture media were renewed with phenol red-free media containing PABA (200 μM), SMZ (200 μM), 4-nitrophenol (4 μM) or DMSO (0.1%) as the solvent control. After 0, 2, 4, 6, and 8 h, the supernatants were collected, mixed with 1 volume of acetonitrile, and incubated on ice for 30 min. In the case of human prostate tissues, for NATs activity determination, the reaction mixtures consisted of human prostate cytosol protein (1 mg/ml) in 25 mM phosphate buffer (pH 7.5) containing 1 mM DTT and PABA (200 μM) or SMZ (500 μM). The reactions were initiated by the addition of AcCoA (1 mM). After 30 min incubation at 37°C, the reactions were terminated by the addition of 1 volume of chilled acetonitrile. For SULT1A1 activity, the reaction mixtures consisted of the cytosolic protein (1 mg/ml), 25 mM phosphate buffer (pH 7.5) containing $MgCl_2$ (10 mM), EDTA (1 mM), and 4-nitrophenol (4 μM). The reactions were initiated by the addition of PAPS (200 μM) and stopped by the addition of 1 volume of chilled acetonitrile after 30 min of incubation at 37°C. All the samples were centrifuged for 10 min at 21 000 × g, and 100 μl of the supernatants were analyzed by HPLC using an Agilent 1260 Infinity model equipped with UV/vis detector. The metabolites were separated with Aquasil C18 column (4.6 × 250 mm, 5 μm particle size) from Thermo Scientific. Separation of PABA from its N-acetylated derivative was performed using a linear gradient of 98% 50 mM acetic acid and 2% acetonitrile ramped to 100% acetonitrile over 20 min at a flow of 1 ml/min. The absorption was monitored at 270 nm with retention times of 8 and 9.5 min for PABA and N-acetyl-PABA, respectively. For SMZ and N-acetyl-SMZ, the chromatography consisted of a linear gradient of 98% 50 mM acetic acid and 2% acetonitrile ramped to 50% acetonitrile over 30 min at a flow of 1 ml/min. The absorbance was monitored at 254 nm with retention times of 15 and 16 min for SMZ and N-acetyl-SMZ, respectively. 4-Nitrophenol and 4-nitrophenylsulfate were resolved with a linear gradient starting at 98% 50 mM ammonium acetate and 2% acetonitrile and ramped to 100% acetonitrile over 20 min at a flow of 1 ml/min. The absorption was monitored at 285 nm with retention times of 8.5 and 10.5 min for 4-nitrophenylsulfate and 4-nitrophenol, respectively. The reactions rates were linear with time and proportional to protein concentration.

The kinase activity was measured in human prostate and LNCaP cytosols using Universal Fluorometric Kinase Assay Kit from Sigma Aldrich following the manufacturer's instructions. Briefly, the kinase reaction was performed at 37°C using the ADP assay buffer (Sigma Aldrich), human prostate, or LNCaP cytosolic protein (1 mg/ml) and ATP (300 μM). After 30 min, the kinase reaction ADP sensor buffer (20 μl) and ADP sensor (10 μl) were added to the reaction mixture and incubated at room temperature for 15 min. The fluorescence intensity corresponding to the ADP moiety was monitored using a plate reader (Synergy H1 plate reader; Biotek) with excitation at 540 nm and emission at 590 nm.

Preparation of human liver, prostate, and LNCaP cytosol and microsomes. The supernatants of the human liver or prostate tissue homogenates (20–25 mg of wet weight of tissue) obtained at 3000 g in TE buffer (50 mM Tris-HCl containing 10 mM EDTA, and 10 mM BME, pH 8.0) were centrifuged consecutively at 9000 × *g* for 20 min and then 100 000 × *g* for 60 min at 4°C using an ultracentrifuge (Beckman Coulter Inc, Brea, California) to obtain cytosolic and microsomal fractions. In the case of LNCaP cells, 10 million cells were homogenized and sonicated in 500 μL of lysis buffer (20 mM Tris-HCL, pH 7.5, 1 mM EDTA, 1 mM DTT, 50 μM PMSF, and 10 μM leupeptin) at 4°C. The cell homogenates were centrifuged at 3000 g for 10 min at 4°C followed by 14 000 × *g* for 60 min at 4°C. Protein concentrations was measured by the Bradford procedure (Bradford, 1976). All fractions were stored at −80°C until use.

CYP1 and CYP1A2 activities. Ethoxyresorufin O-deethylase (EROD) and methoxyresorufin O-demethylase (MROD) activity associated with CYP1 and CYP1A2, respectively (Burke and Mayer, 1983; Eugster *et al*., 1993), were measured in human prostate microsomes and LNCaP cytosols. The reaction mixture consisted of 100 mM phosphate buffer pH 7.4 containing microsomal protein or LNCaP cytosol (1 mg/ml), EDTA (0.1 mM), $MgCl_2$ (5 mM), NADPH (1 mM), and ethoxyresorufin or methoxyresorufin (5 μM). The reaction was conducted at 37°C over 30 min. Resorufin formation was monitored by fluorescence employing a plate reader (Synergy H1 plate reader; Biotek) with excitation at 530 nm and emission at 585 nm, over 5-min intervals for 30 minutes of reaction.

DNA binding assays. AcCoA-dependent binding of HONH-PhIP to CT-DNA was performed at 37°C under an atmosphere of argon, in 25 mM phosphate buffer, pH 7.5, containing CT-DNA (1 mg/ml), DTT (1 mM), human prostate cytosols or LNCaP cytosols (1 mg/ml) or recombinant human NAT1 and NAT2 (1 mg/ml), AcCoA (1 mM), and HONH-PhIP (0.1 or 1 μM). PAPS-dependent DNA binding catalyzed by sulfotransferases was performed at 37°C under argon in 25 mM phosphate buffer, pH 7.5, containing CT-DNA (1 mg/ml), $MgCl_2$ (10 mM), EDTA (1 mM), prostate cytosolic protein or LNCaP cytosols (1 mg/ml), PAPS (0.2 mM), and HONH-PhIP (0.1 or 1 μM). ATP-dependent DNA binding of HONH-PhIP (0.1 or 1 μM) catalyzed by kinases was performed under the same conditions as PAPs except that ATP (1 mM) was employed as the cofactor. All reactions were done in a final volume of 0.125 ml. The reactions were terminated after 30 min of incubation by the addition of 2 volumes of ethyl acetate. After centrifugation at 21 000 × *g* for 10 min, the aqueous phase was retrieved and the DNA was precipitated by the addition of 0.1 volume of NaCl (5 M) and 2 volumes of chilled isopropanol. After washing the pelleted DNA with 70% ethanol, the DNA was dried and reconstituted in 5 mM Bis-Tris buffer (pH 7.1) and digested in the presence of internal standards (1 adducts per 10^7 DNA bases) (Nauwelaers, *et al*., 2011).

Statistics. Statistical evaluation was performed using Prism 5.03 (GraphPad Software, La Jolla, California). The statistical significance was determined by the Student's *t*-test to determine the effect of treatment within a group. The data are presented as the mean ± SD ($^*p < .05$; $^{**}p < .01$, $^{***}p < .005$ vs control).

RESULTS

dG-C8-PhIP Is Detected in Human Prostate

DNA adducts derived from PhIP, MeIQx, and AαC were screened in 54 human prostate DNA obtained from PC patients. dG-C8-PhIP was detected in 13 of 54 samples. In contrast, DNA adducts of the other chemicals were not detected (<0.3 adducts per 10^8 DNA bases). dG-C8-PhIP was detected in both transition and peripheral zones and occurred at comparable levels, ranging between 0.2 and 12 adducts per 10^8 bases (Figure 1).

Cytotoxicity of HAAs and HONH-HAAs in LNCaP Cells

The cytotoxicity induced by HAAs and their HONH-HAA metabolites was evaluated in LNCaP cells by the MTS assay. As shown in Figure 2A, the treatment of the LNCaP cells with each of the 4 HAAs (1–10 μM) for 24 h had no effect on the cell viability. However, when the cells were treated with HONH-HAAs, a concentration-dependent cytotoxicity was induced by HONH-PhIP (Figure 2B), whereas cytotoxicity was not observed when the cells were treated with HONH-MeIQx, HONH-IQ, or HONH-AαC.

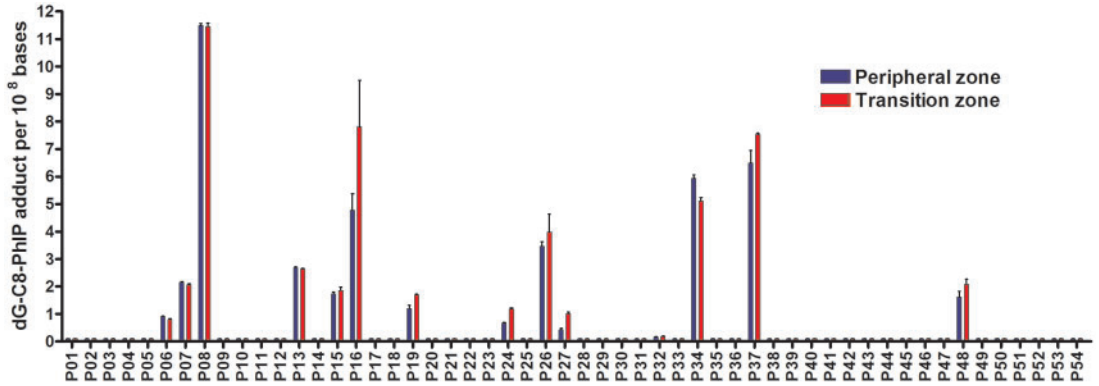

Figure 1. dG-C8-PhIP levels in human prostate peripheral and transition zones. dG-C8-PhIP were measured by UPLC-ESI/MS^3. dG-C8-PhIP adduct levels are expressed as adducts per 10^8 bases. Abbreviations: dG-C8-PhIP, N-(2′-deoxyguanosin-8-yl)-PhIP; PhIP, 2-amino-1-methyl-6-phenylimidazo[4,5-*b*]pyridine; UPLC-ESI/MS^3, ultraperformance liquid chromatography-electrospray ionization multistage scan mass spectrometry.

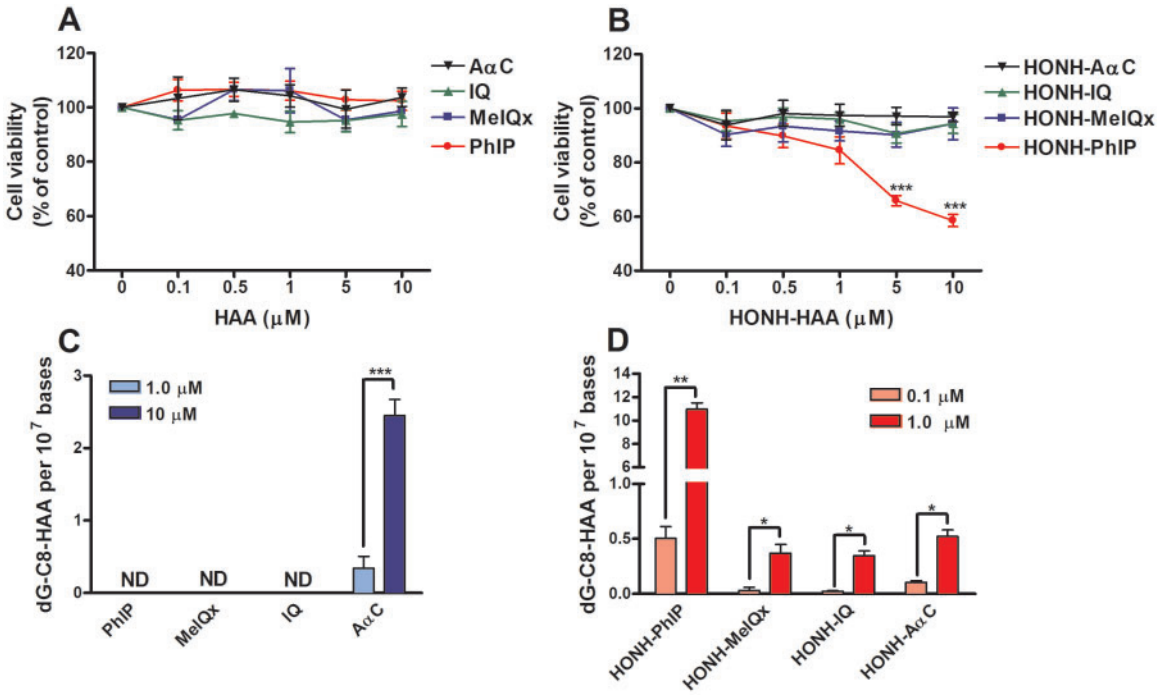

Figure 2. HAAs and HONH-HAAs cytotoxicity and DNA adduct formation in LNCaP cells. (A and B) Cytotoxicity of HAAs and HONH-HAAs in LNCaP cells. After 24 h of treatment with either DMSO (0.1%), HAAs, or HONHHAAs (0.1 μM – 10 μM), the LNCaP cell viability was evaluated by the MTS assay. (C and D) HAAs and HONH-HAAs DNA adducts formation in LNCaP cells. After 24 h of treatment with PhIP, MeIQx, IQ, and AαC, DNA adducts were measured by UPLC-ESI/MS^3. Data are representative of at least three different experiment and are expressed as mean ± SD. (Two-tail student's t-test, $^*P < .05$; $^{**}P < .01$, $^{***}P < .005$ versus control). Abbreviations: AαC, 2-amino-9*H*-pyrido[2,3-*b*]indole; Ctrl, control; DMSO, dimethyl sulfoxide; HAA, heterocyclic aromatic amine; HNOH-HAA, N-hydroxy-HAA; LNCaP, human prostate cell line; IQ, 2-amino-3-methylimidazo[4,5-*f*]quinoline; MeIQx, 2-amino-3,8-dimethylmidazo[4,5-*f*]quinoxaline; ND, not detected; PhIP, 2-amino-1-methyl-6-phenylimidazo[4,5-*b*]pyridine; UPLC-ESI/MS^3, ultraperformance liquid chromatography-electrospray ionization multistage scan mass spectrometry.

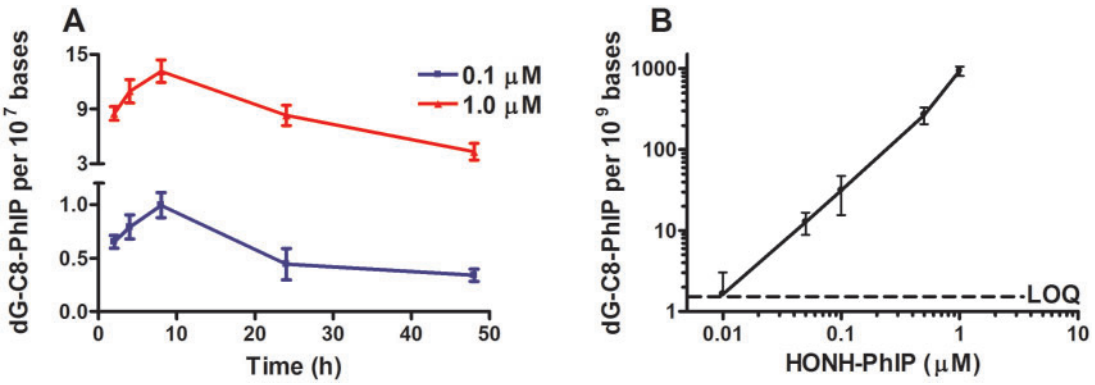

Figure 3. Kinetic and dose effect on the formation of dG-C8-PhIP in LNCaP cells. (A) Kinetics of dG-C8-PhIP formation in LNCaP cells. After 2, 4, 8, 24, and 48 h of treatment with 0.1 μM or 1μM of HONH-PhIP, dG-C8-PhIP formed were measured by UPLC-ESI/MS^3. (B) dG-C8-PhIP formation in LNCaP cells as function as HONH-PhIP concentrations. After 8 h of treatment with HONH-PhIP (0.1 nM – 1 μM), dG-C8-PhIP formed in LNCaP cells were measured by UPLC-ESI/MS^3. Data are representative of at least three-different experiments and are expressed as mean ± SD. (Two-tail student's t-test, *$P < .05$; **$P < .01$, ***$P < .005$ versus Ctrl). Abbreviations: Ctrl, control; HNOH-PhIP, 2-hydroxy-amino-1-methyl-6-phenylimidazo[4,5-*b*]pyridine; LOQ, limit of quantification; LNCaP, human prostate cell line; dG-C8-PhIP, *N*-(2′-deoxyguanosin-8-yl)-PhIP; PhIP, 2-amino-1-methyl-6-phenylimidazo[4,5-*b*]pyridine; UPLC-ESI/MS^3, ultraperformance liquid chromatography-electrospray ionization multistage scan mass spectrometry.

HAA-DNA Adducts Formation in LNCaP Cells

The DNA adducts formed by PhIP, MeIQx, IQ and AαC, and their HONH-HAA derivatives were measured after 24 h of cell treatment with HAAs (1 or 10 μM) or with HONH-HAAs (0.1 or 1 μM). As illustrated in Figure 2C, DNA adducts were detected in LNCaP after treatment with AαC, but DNA adducts were not detected with PhIP, MeIQx or IQ. The levels of dG-C8-AαC increased in a concentration-dependent manner and ranged between 0.3 and 2 adduct per 10^7 bases. Given the low levels of CYP activity in LNCaP cells (*vide infra*), we surmise that the bioactivation and DNA binding of AαC occurred by a non-CYP oxidase. (Turesky *et al.*, 2015). In contrast, when LNCaP cells were treated with HONH-HAAs, DNA adducts of all HAAs were detected (Figure 2D). The levels of DNA adducts formed by HONH-MeIQx, HONH-IQ, and HONH-AαC were comparable; however, those formed by HONH-PhIP were ~20-fold higher. Representative UPLC-ESI/MS^3 chromatograms are shown in Supplementary Information data (Supplementary Figure 1).

Time- and Concentration-Dependent Formation of dG-C8-PhIP in LNCaP Cells

The kinetics of dG-C8-PhIP formation was characterized in LNCaP cells after treatment with either 0.1 or 1 μM of HONH-PhIP. As shown in Figure 3A, dG-C8-PhIP was formed within 2 h of treatment, and the level reached a maximum at 8 h, before starting to decrease over the ensuing 24 and 48 h. The decrease in dG-C8-PhIP levels may be a result of DNA repair and/or cell division and requires investigation.

We also determined the formation of dG-C8-PhIP as a function of HONH-PhIP concentration. The levels of dG-C8-PhIP were measured after 8 h of treatment of LNCaP cells at concentrations ranging from 1 nM to 1 μM of HONH-PhIP. An exposure period of 8 h was chosen for the study based on the previous experiment, where the highest levels of dG-C8-PhIP were formed at this time point. dG-C8-PhIP formation occurred in a concentration-dependent manner, and DNA adducts were detected at a concentration as low as 5 nM HONH-PhIP (Figure 3B).

Kinetic Studies on the Stability and Metabolism of HONH-PhIP and HONH-MeIQx in LNCaP Cells

We examined the stability of HONH-PhIP and HONH-MeIQx, and their metabolic fates in LNCaP cells, to determine whether greater stability and bioavailability of HONH-PhIP could explain its capacity to form higher levels of DNA adducts compared to other HONH-HAAs. As reported in Figure 4, both HONH-PhIP and HONH-MeIQx underwent reduction to the parent amines. The half-lives of HONH-PhIP and HONH-MeIQx were estimated at, respectively, 3.0 and 2.3 h. There was no evidence for the formation of ring-oxidized metabolites or Phase II conjugates for either HONH-HAA or their reduced parent amines as measured by HPLC UV detection (Turesky and Le Marchand, 2011). These findings reveal that enzymatic reduction is the principal metabolic pathway of HONH-PhIP and HONH-MeIQx in LNCaP cells; this reduction step competes with Phase II enzymes involved in the bioactivation of HONH-HAAs. King *et al.* identified an NADH-dependent reductase activity in rodent and human liver microsomes that rapidly converted HONH-arylamines and HONH-HAAs back to the parent amines (King *et al.*, 1999). This reaction serves as a mechanism of detoxification and limits the bioavailability of the HONH-HAAs for further bioactivation by Phase II enzymes. However, the modest differences between the half-lives of HONH-PhIP and HONH-MeIQx does not seem to explain the >20-fold differences in DNA adduct levels formed by these 2 HONH-HAAs in LNCaP cells. Further studies are required to examine the potential role of NADH-dependent reductase in HAA-DNA adduct formation in prostate.

Phase II Enzyme Functional Activity in LNCaP Cells

We characterized the activities of SULT1A1, NATs (NAT1 and NAT2), and UDP-glucuronosyltransferase 1A1 (UGT1A1 and UGT1A9), enzymes that are involved in the metabolism of HONH-PhIP (Turesky and Le Marchand, 2011). The enzymatic activities of SULT1A1, NAT1, NAT2 UGT1A1 and UGT1A9 were characterized using their specific substrates, 4-nitrophenol, PABA, SMZ, β-estradiol, and propofol, respectively, in intact LNCaP cells (Donato *et al.*, 2010; Grant *et al.*, 1991; Tabrett and Coughtrie, 2003). The highest enzyme activity was observed for NAT1 (1.64 ± 0.25 nmol/min/mg protein), followed by SULT1A1 (0.46 ± 0.08 nmol/min/mg protein), and NAT2 (0.07 ± 0.02 nmol/min/mg protein; Table 1). In contrast, UGT1A1 and UGT1A9 activities were not detected (limits of detection were 1.0 and 3.5 pmol/min/mg of protein for UGT1A1 and UGT1A9, respectively). These data are in agreement with a study reporting low

levels of messenger RNA (mRNA) and protein expression of UGT1A1 and UGT1A9 in LNCaP cells (Takayama *et al.*, 2007).

The Effect of PCP on dG-C8-PhIP Formation in LNCaP Cells

The role of SULTs in the bioactivation of HONH-PhIP in LNCaP cells was assessed with PCP, a known inhibitor of SULTs (Meerman *et al.*, 1980). The levels of dG-C8-PhIP decreased in a concentration-dependent manner in LNCaP cells co-treated with 0.1 μM of HONH-PhIP and variable amounts of PCP (1.25–20 μM; Figure 5A). dG-C8-PhIP formation was reduced by up to 75% by PCP and was associated with a significant concentration-dependent decrease in enzymatic activity, measured by the sulfation of 4-nitrophenol as a substrate for SULT1A1 activity (Figure 5B), suggesting the involvement of SULT1A1 in the bioactivation of HONH-PhIP. Since the bioactivation of HONH-PhIP can also be carried out by NATs (Turesky and Le Marchand, 2011), the effect of PCP on NAT1 and NAT2 activities was also assessed in LNCaP cells. As shown in Figure 5C, PCP treatment also led to a significant concentration-dependent decrease in NAT1 and NAT2 activities, based on N-acetylation of PABA and SMZ, respectively, demonstrating that PCP is an inhibitor of both NAT1 and NAT2. Thus, HONH-PhIP undergoes further biotransformation in LNCaP cells to form the presumed reactive N-sulfooxy and N-acetoxy esters that bind to DNA and form adducts.

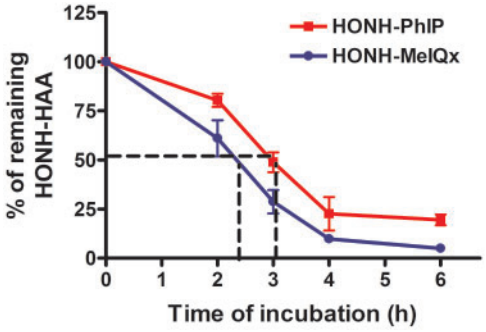

Figure 4. HONH-PhIP and HONH-MeIQx half-life estimates in LNCaP cells. LNCaP cells were treated with HONH-PhIP or HONH-MeIQx (1μM) and the remaining HONH-HAAs were measured after of 0, 2, 3, 4 and 6 h of incubation by HPLC. Abbreviations: HAA, heterocyclic aromatic amine; HONH-HAA, N-hydroxy-HAA HONH-PhIP, 2-hydroxy-amino-1-methyl-6-phenylimidazo[4,5-*b*]pyridine; LNCaP, human prostate cell line; HONH-MeIQx, 2-hydroxy-amino-3,8-dimethylmidazo[4,5-*f*]quinoxaline; HPLC, high-performance liquid chromatography.

The Effect of Mefenamic Acid on dG-C8-PhIP Formation in LNCaP Cells

We further examined the role of SULT1A1 in bioactivation of HONH-PhIP in LNCaP cells using mefenamic acid, a nonsteroidal anti-inflammatory drug reported to be a specific inhibitor for SULT1A1 (Vietri *et al.*, 2000). As shown in Figure 6B, the treatment of cells with increasing concentrations of mefenamic acid (1–10 μM) results in a strong to complete inhibition of SULT1A1 activity, based on the sulfation of 4-nitrophenol. Moreover, mefenamic acid treatment had no effect on NAT1 and NAT2 activities. Thus, in contrast to PCP, mefenamic acid is a strong and a specific inhibitor of SULT1A1. The presence of increasing concentrations of mefenamic acid showed a significant concentration-dependent decrease in the levels of dG-C8-PhIP (Figure 6A). However, compared to PCP, the effectiveness of mefenamic acid to diminish SULT-mediated DNA binding of PhIP was appreciably lower. Taken together, these data imply SULT1A1 contributes to about 25% of dG-C8-PhIP formation.

Rhod-o-hp Effect on dG-C8-PhIP Formation in LNCaP Cells

Rhod-o-hp is a benzylidenerhodanine derivative and an inhibitor of both NAT1 and NAT2 (Russell *et al.*, 2009; Tiang *et al.*, 2010). We used Rhod-o-hp to probe the contribution of NATs in the bioactivation of HONH-PhIP in LNCaP cells. As shown in Figure 6C, increasing concentrations of Rhod-o-hp significantly decreased the levels of dG-C8-PhIP. However, we observed that Rhod-o-hp also inhibits SULT1A1 activity, a previously unreported effect of this compound. The diminution in the level of dG-C8-PhIP in LNCaP cells treated with Rhod-o-hp was similar to the decrease in adduct levels when cells were challenged with PCP. Rhod-o-hp is a more potent inhibitor of NAT2 than NAT1. The NAT1 activity remaining in the presence of 150 μM Rhod-o-hp was about 75% of the control and 4-fold higher than the remaining NAT2 activity. Under this concentration of inhibitor, there was a modest but significant ~25% decrease in the level of dG-C8-PhIP. The stronger inhibitory effect of Rhod-o-hp on NAT2 is suggestive of a more prominent role for NAT1 in bioactivation of HONH-PhIP in LNCaP cells. However, the

Table 1. Phase I and Phase II Enzymes Activities in LNCaP Cells and Human Prostate Cytosols

	pmol/min/mg Protein		nmol/min/mg Protein					
	CYP1 (EROD)	CYP1A2 (MROD)	NAT1 (PABA)	NAT2 (SMZ)	SULT1A1 (4-nitrophenol)	UGT1A1 (β-estradiol)	UGT1A9 (propofol)	Kinase
LNCaP	0.25 ± 0.09	ND	1.64 ± 0.25	0.07 ± 0.02	0.46 ± 0.08	ND	ND	3.08 ± 0.22
Human prostate 1	0.29 ± 0.09	ND	0.27 ± 0.04	ND	0.02 ± 1.05	NA	NA	1.08 ± 1.86
Human prostate 2	0.30 ± 0.08	ND	1.05 ± 0.01	ND	0.01 ± 1.33	NA	NA	0.47 ± 0.30
Human prostate 3	0.30 ± 0.09	ND	1.86 ± 0.01	ND	0.02 ± 0.21	NA	NA	1.38 ± 1.62
Human prostate 4	0.35 ± 0.11	ND	2.11 ± 0.07	ND	0.03 ± 0.04	NA	NA	2.13 ± 1.04
Human liver 1	31.61 ± 3.56	28.12 ± 1.97	NA	NA	NA	NA	NA	NA
Human liver 2	18.43 ± 3.10	19.70 ± 2.64	NA	NA	NA	NA	NA	NA
Human liver 3	46.29 ± 7.20	28.11 ± 2.08	NA	NA	NA	NA	NA	NA
Human liver 4	23.41 ± 3.34	13.44 ± 0.87	NA	NA	NA	NA	NA	NA
Human recombinant NAT1	NA	NA	230	NA	NA	NA	NA	NA
Human recombinant NAT2	NA	NA	NA	210	NA	NA	NA	NA

Abbreviations: EROD, Ethoxyresorufin O-deethylase; LNCaP, human prostate cell line; MROD, methoxyresorufin O-demethylase; ND, not detected; NA, not assayed; NAT1, N-acetyltransferase 1; NAT2, N-acetyltransferase 2; PABA, 4-aminobenzoic acid; SMZ, sulfamethazine; SULT1A1, sulfotransferase 1A1.
The limits of detection are 0.2 pmol/min/mg of protein (MROD), 1.3 pmol/min/mg protein (NAT2), 1 pmol/min/mg (UGT1A1), and 3.5 pmol/min/mg of protein (UGT1A9).

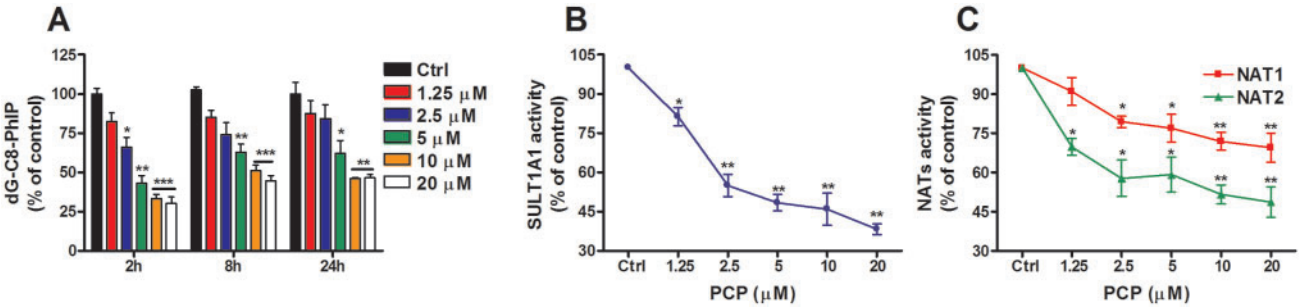

Figure 5. PCP effect on dG-C8-PhIP and Phase II enzymes activity in LNCaP cells. (A) Effect of PCP on dG-C8-PhIP formation in LNCaP cells. Cells were co-treated with HONH-PhIP (0.1 μM) and PCP (0- 20 μM). After 2, 8, and 24 h of treatment, dG-C8-PhIP formed in LNCaP cells were measured by UPLC-ESI/MS^3. (B) Effect of PCP on SULT1A1 activity in LNCaP cells. Cells were co-treated with 4-nitrphenol (4 μM) and PCP (0 - 20 μM). After 8 h of treatment, 4-nitrophenylsulfate formation was monitored by HPLC. (C) Effect of PCP on NAT1 and NAT2 activities in LNCaP cells. Cells were co-treated with PABA (200 μM) or SMZ (200 μM) and PCP (0- 20 μM). After 8 h of treatment, N-acetylated PABA and N-acetylated SMZ were measured by HPLC. Data are representative of three different experiments and are expressed as the mean ± SD. (Two-tail student's t-test, $^*P < .05$; $^{**}P < .01$, $^{***}P < .005$ versus ctrl). Abbreviations: Ctrl, control; dG-C8-PhIP, *N*-(2′-deoxyguanosin-8-yl)-PhIP; HONH-PhIP, 2-hydroxy-amino-1-methyl-6-phenylimidazo[4, 5-*b*]pyridine; HPLC, high-performance liquid chromatography; LNCaP, human prostate cell line; NAT1, N-acetyltransferase 1; NAT2, N-acetyltransferase 2; PhIP, 2-amino-1-methyl-6-phenylimidazo[4,5-*b*]pyridine; PABA, 4-aminobenzoic acid; SMZ, sulfamethazine; PCP, pentachlorophenol; SULT1A1, sulfotransferase 1A1; UPLC-ESI/MS^3, ultraperformance liquid chromatography-electrospray ionization multistage scan mass spectrometry.

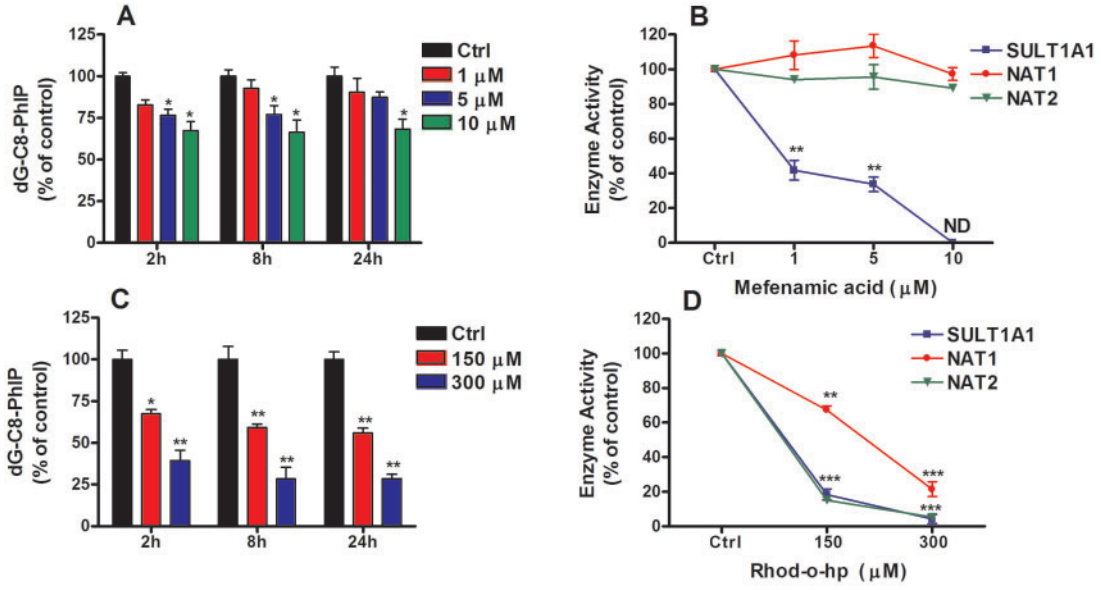

Figure 6. The effects of mefenamic and Rho-o-hp on dG-C8-PhIP formation and Phase II enzyme activities in LNCaP cells. (A) Effect of mefenamic acid on dG-C8-PhIP formation in LNCaP cells. Cells were co-treated with HONH-PhIP (0.1 μM) and mefenamic acid (0 - 10 μM). After 2, 8, and 24 h of treatment, dG-C8-PhIP formed in LNCaP cells were measured by UPLC-ESI/MS^3. (B) Effect of mefenamic acid on SULT1A1, NAT1, and NAT2 activities in LNCaP cells. Cells were co-treated with 4-nitrphenol (4 μM), PABA (200 μM), or SMZ (200 μM) and mefenamic acid (0- 10 μM). After 8 h of treatment, 4-nitrophenylsulfate, N-acetyl-PABA, and N-acetyl-SMZ formation were measured by HPLC. (C) Effect of Rho-o-hp on dG-C8-PhIP formation in LNCaP cells. Cells were co-treated with HONH-PhIP (0.1 μM) and Rho-o-hp (0- 300 μM). After 2, 8, and 24 h of treatment, dG-C8-PhIP formed in LNCaP cells were measured by UPLC-ESI/MS^3. (D) Effect of Rho-o-hp on SULT1A1, NAT1 and NAT2 activities in LNCaP cells. Cells were co-treated with 4-nitrphenol (4 μM), PABA (200 μM), or SMZ (200 μM) and Rho-o-hp (0 - 300 μM). After 8 h of treatment, 4-nitrophenylsulfate, N-acetyl-PABA, and N-acetyl-SMZ formation were monitored by HPLC. Data are representative of three different experiment and are expressed as the mean ± SD. (Two-tail student's t-test, $^*P < .05$; $^{**}P < .01$, $^{***}P < .005$ versus control). Abbreviations: Ctrl, control; dG-C8-PhIP, *N*-(2′-deoxyguanosin-8-yl)-PhIP; HONH-PhIP, 2-hydroxy-amino-1-methyl-6-phenylimidazo[4,5-*b*]pyridine; HPLC, high-performance liquid chromatography; LNCaP, human prostate cell line; NAT1, N-acetyltransferase 1; NAT2, N-acetyltransferase 2; PhIP, 2-amino-1-methyl-6-phenylimidazo[4,5-*b*]pyridine; PABA, 4-aminobenzoic acid; SMZ, sulfamethazine; PCP, pentachlorophenol; Rho-o-hp, (Z)-5-(2′-hydroxybenzylidene)-2-thioxothiazolidin-4-one; SULT1A1, sulfotransferase 1A1; UPLC-ESI/MS^3, ultraperformance liquid chromatography-electrospray ionization multistage scan mass spectrometry.

mechanism of NATs inhibition by Rhod-o-hp has not been characterized, and the relative contributions of NAT1 and NAT2 in bioactivation of HONH-PhIP should be interpreted with caution. Collectively, these inhibition studies suggest that the SULT1A1 and NATs enzymes account for, respectively, about 25% and 50% of the HONH-PhIP binding to DNA in LNCaP cells (Figure 6D).

Metabolic Activation of HONH-PhIP in LNCaP Cytosols

The bioactivation of HONH-PhIP to reactive DNA binding intermediates was also assessed in the cytosolic fraction of LNCaP cells fortified with AcCoA or PAPS, the cofactors of NATs and SULTs, respectively. Boiled cytosols served as the negative controls in the presence of cofactors, since the cofactors alone may react nonenzymatically to HONH-PhIP and augment the level of its DNA binding. As shown in Figure 7, both cofactors alone led to a significant increase in dG-C8-PhIP formation at both doses of HONH-PhIP (0.1 and 1 μM). The cytosols fortified with AcCoA resulted in a 10-fold greater level of dG-C8-PhIP formation compared to cytosols fortified with PAPS. We also measured the bioactivation of HOHN-PhIP in the presence of ATP, since 2 studies

suggested a potential bioactivation of HONH-HAAs by kinases (Agus *et al.*, 2000; Nelson *et al.*, 2001). Our data show that cytosolic kinases do lead to a bioactivation of HONH-PhIP; however, the levels of dG-C8-PhIP formed are much lower than the DNA binding of HONH-PhIP in cytosols fortified with AcCoA or PAPS (Figure 7). Collectively, these data point to NATs as the major conjugation enzymes in the bioactivation of HONH-PhIP in LNCaP cells.

CYP1A1, CYP1B1, CYP1A2, and Phase II Activities in Human Prostate

We assessed the functional activities of CYP1A1, CYP1B1 and CYP1A2, enzymes that are involved in the metabolism of PhIP (Turesky and Le Marchand, 2011). MROD activity, which is selective for CYP1A2 (Eugster, *et al.*, 1993), was not detected in human prostate microsomes (< 0.2 pmol/min/mg of protein), whereas low but measurable activity was detected for EROD, a general substrate for CYP1 family isoforms (up to 0.3 pmol/min/mg of protein; Table 1; Burke and Mayer, 1983). However, the EROD activity in human prostate microsomes was 60- to 150-fold lower than the activity observed with human liver microsomes (Table 1).

The functional activities of Phase II enzymes including SULT1A1, NAT1 and NAT2, and kinases, were determined with human prostate cytosols. As reported in Table 1, NAT2 activity was not detectable (<1.3 pmol/min/mg protein); however, significant NAT1 activity was detected in all samples. The rate of PABA N-acetylation ranged from 0.3 to 2.1 nmol/min/mg of protein. SULT1A1 activity was also detected in all human prostate cytosols with rates of sulfation of 4-nitrophenol ranging between 8.7 and 29 pmol/min/mg of protein.

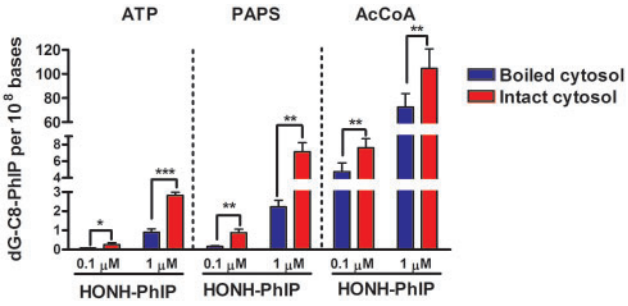

Figure 7. HONH-PhIP bioactivation in LNCaP cytosols. HONH-PhIP (0.1 μM or 1 μM) was incubated in intact or boiled LNCaP cytosols containing CT-DNA in the presence of AcCoA, PAPS, or ATP. After 30 min of incubation, the dG-C8-PhIP formed were measured by UPLC-ESI/MS^3. Data are representative of four different experiments and are expressed as the mean ± SD. (Two-tail student's t-test, *$P < .05$; **$P < .01$, ***$P < .005$ versus control). Abbreviations: ATP, adenosine 5-triphosphate; AcCoA, acetyl coenzyme A; Ctrl, control; CT-DNA, calf thymus DNA; dG-C8-PhIP, *N*-(2′-deoxyguanosin-8-yl)-PhIP; HONH-PhIP, 2-hydroxy-amino-1-methyl-6-phenylimidazo[4,5-*b*]pyridine; LNCaP, human prostate cell line; PAPS, adenosine 3-phosphate 5-phosphosulfate; UPLC-ESI/MS^3, ultraperformance liquid chromatography-electrospray ionization multistage scan mass spectrometry.

Metabolic Activation of HONH-PhIP in Human Prostate Cytosols

O-Acetyltransferase and sulfotransferase-dependent bioactivation of HONH-PhIP were determined in human prostate cytosols in the presence of AcCoA or PAPS. As shown in Figure 8, DNA binding of HONH-PhIP was enhanced by both cofactors at both concentrations of HONH-PhIP (0.1 and 1 μM). However, the levels of dG-C8-PhIP formed by cytosols in the presence of AcCoA were 10- to 200-fold higher than those levels formed in the presence of PAPS, employing the same concentrations of HONH-PhIP. We also assessed the role of the kinases in the bioactivation of HONH-PhIP in human prostate cytosol. The presence of ATP as a cofactor resulted in an increase in dG-C8-PhIP adduct formation for both concentrations of HONH-PhIP (0.1 and 1 μM); however, the levels of dG-C8-PhIP adduct remained much lower than those levels formed by cytosols fortified with PAPS or AcCoA (Figure 8).

Metabolic Activation of HONH-PhIP by Human Recombinant NAT1 and NAT2

The bioactivation of HONH-PhIP to reactive DNA binding intermediates, by human NAT1 and NAT2, was also assessed using human recombinant enzymes. As shown in Supplementary Figure 3, the bioactivation of HONH-PhIP was efficiently carried out by both enzymes. However, the rates of NAT2 bioactivation, measured by dG-C8-PhIP adduct formation, were 30- to 40-fold higher than for NAT1.

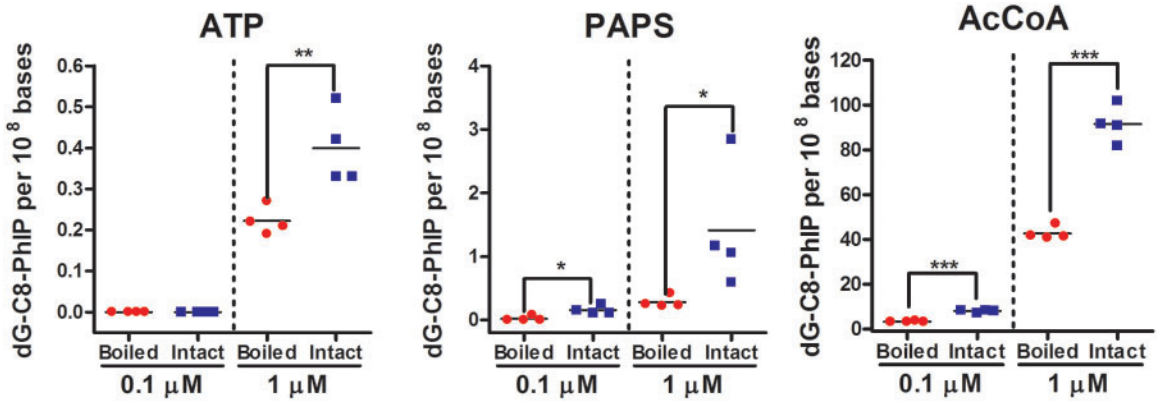

Figure 8. HONH-PhIP bioactivation in human prostate cytosolic fractions. HONH-PhIP (0.1 μM or 1 μM) was incubated with intact or boiled human prostate cytosols of four patients in the presence of CT-DNA and the cofactors AcCoA, PAPS, or ATP. After 30 min of incubation, the amount of dG-C8-PhIP formed was measured by UPLC-ESI/MS^3. Data are representative of four different experiments and are expressed as the mean ± SD. (One-tail student's Student's t-test, *$P < .05$; **$P < .01$, ***$P < .005$ versus control). Abbreviations: ATP, adenosine 5-triphosphate; AcCoA, acetyl coenzyme A; Ctrl, control; CT-DNA, calf thymus DNA; dG-C8-PhIP, *N*-(2′-deoxyguanosin-8-yl)-PhIP; HONH-PhIP, 2-hydroxy-amino-1-methyl-6-phenylimidazo[4,5-*b*]pyridine; LNCaP, human prostate cell line; PAPS, adenosine 3-phosphate 5-phosphosulfate; UPLC-ESI/MS^3, ultraperformance liquid chromatography-electrospray ionization multistage scan mass spectrometry.

DISCUSSION

PhIP is the only HAA studied shown to induce PC in rodent models and thus far the only HAA found to form DNA adducts in human prostate (Xiao, *et al.*, 2016). We have now detected dG-C8-PhIP in 13 of the 54 patients screened. These emerging biomarker data support the paradigm that consumption of well-done cooked meat containing PhIP plays a role in DNA damage of the prostate and a plausible role of PhIP in the etiology of PC (Bouvard *et al.*, 2015).

We employed LNCaP cells to examine the cytotoxicity and DNA adduct formation of several HAAs formed in cooked meat. None of the HAAs were toxic, and only AαC formed DNA adducts, possibly through metabolic activation by a non-CYP oxidase (Turesky *et al.*, 2015). HONH-PhIP, but not the other HONH-HAAs, induced cytotoxicity. Moreover, the levels of dG-C8-PhIP in LNCaP cells were 20-fold or greater than the adduct levels formed with other HONH-HAAs. dG-C8-PhIP formation in LNCaP cells occurred as a linear function of dose over a 1000-fold exposure range of HONH-PhIP down to a concentration of 10 nM a concentration approaching the exposure to PhIP in the diet (Bogen *et al.*, 2007). These data indicate that the CYP-mediated N-oxidation step of HAAs likely occurs in liver, followed by systemic circulation of the HONH-HAAs to the prostate, where further bioactivation by Phase II enzymes can occur (Scheme 2) (Turesky and Le Marchand, 2011). The higher susceptibility of human LNCaP cells to the DNA-damaging effects of PhIP compared to other prominent HAAs in cooked meats recapitulates our DNA adduct biomarker data in the prostate genome of PC patients (Xiao, *et al.*, 2016).

The poor N-oxidation of HAAs in LNCaP cells and prostate tissues is due to the very low or lack of expression of CYP1 enzymes (Table 1). Our results are in accordance with previous reports showing a nondetectable to a very low mRNA and protein expression of CYP1A1, CYP1B1. and CYP1A2 and EROD activity in LNCaP cells (Hruba *et al.*, 2010; Kizu *et al.*, 2003). We also show that human prostate tissues harbor low CYP1 activity, based on EROD, but nondetectable CYP1A2 activity, based on MROD activity. These results are consistent with previous studies reporting low levels of mRNA expression of CYP1A1, CY1A2, and CYP1B1 in human prostate (Di Paolo *et al.*, 2005; John *et al.*, 2009; Martin *et al.*, 2010). To our knowledge, functional CYP1 activity in prostate has not been reported previously.

Wang et al. reported that HONH-PhIP formed 50- to 100-fold higher levels of DNA adducts than formed by HONH-MeIQx in primary human prostate cells (Wang *et al.*, 1999). They proposed that the large discrepancy between reactivity of HONH-PhIP and HONH-MeIQx with DNA in prostate cells was attributed to a 10-fold shorter half-life for HONH-MeIQx compared to HONH-PhIP based on a kinetics study of the HONH-HAAs in neutral saline (Wang, *et al.*, 1999). However, we carefully examined the metabolic fate of HONH-PhIP and HONH-MeIQx in LNCaP cells and showed that their half-lives were between 3 and 2.3 h, respectively, and unlikely to be the reason for >20-fold higher levels of HONH-PhIP binding to DNA in LNCaP cells. Hence, the difference in DNA binding of these 2 HONH-HAAs may be explained by differences in their bioactivation pathways. However, LNCaP cells lack several Phase II enzymes involved in the detoxification of HONH-HAAs, including UGTs and Glutathione S-transferases (Dubey and Owusu-Apenten, 2014). HONH-PhIP is reduced to its parent amine by GST or it undergoes conjugation by UGTs, a major enzyme detoxification pathway of HONH-PhIP (Scheme 2; Turesky and Le Marchand, 2011). The absence of these Phase II enzymes in LNCaP cells may increase the

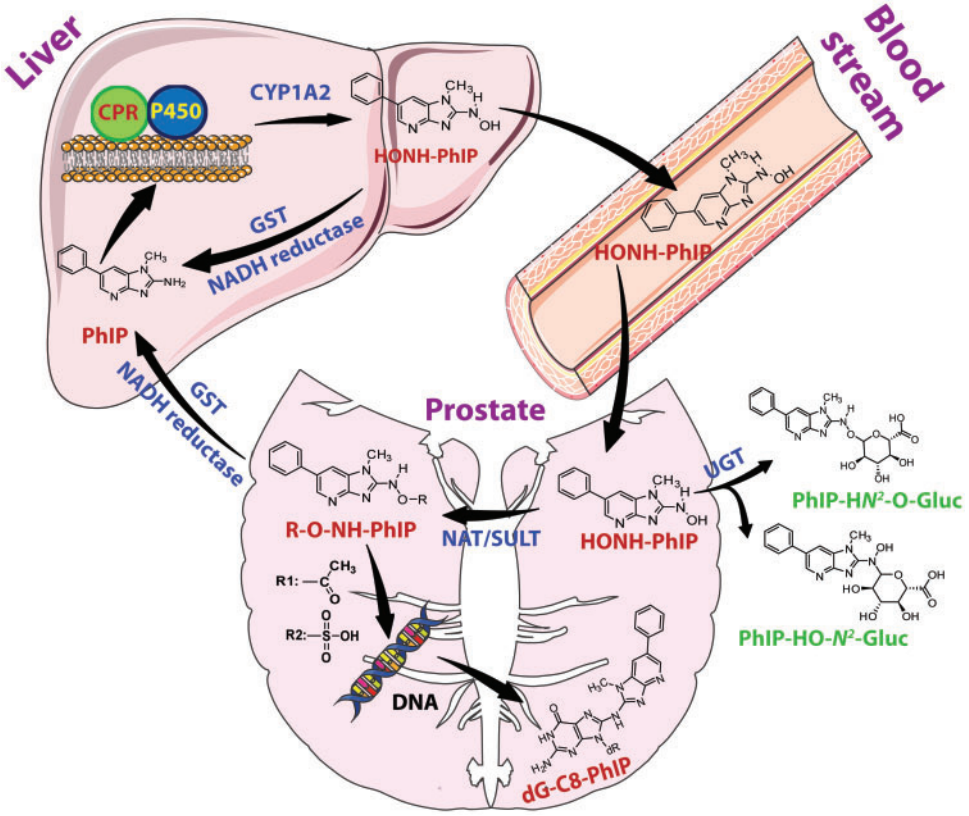

Scheme 2. Metabolism of PhIP and DNA adduct formation in prostate.

bioavailability of HNONH-PhIP and its reactivity with DNA. Thus, data on cytotoxicity and DNA adduct formation of HONH-HAAs in LNCaP cells should be interpreted with caution.

The formation of dG-C8-PhIP in LNCaP cells requires bioactivation of NHOH-PhIP to reactive Phase II intermediates such as the N-sulfooxy and N-acetoxy conjugates (Scheme 2). Mefenamic acid, a specific SULT1A1 inhibitor (Vietri, *et al.*, 2000), resulted in a complete inhibition of SULT1A1 activity and led to a 25% decrease in the level of dG-C8-PhIP. When PCP or Rhod-o-hp, inhibitors of both SULT1A1 and NATs, were used for study, the DNA binding of PhIP decreased by about 75%. Thus, the relative contribution SULT1A1 and NATs in dG-C8-PhIP formation is about 25% and 50%, respectively. The contribution of SULT1A1 to the bioactivation of HONH-PhIP is consistent with data obtained with *Salmonella typhimurium* strains and V79 cells expressing SULT1A1 (Chevereau *et al.*, 2017; Muckel *et al.*, 2002).

We sought to determine the relative contributions of NAT1 and NAT2 in the bioactivation of HONH-PhIP. PABA and SMZ are highly selective substrates for NAT1 and NAT2, respectively (Grant, *et al.*, 1991) and were used as competitive inhibitors of NAT1 and NAT2. The co-incubation of both compounds with HONH-PhIP resulted in a significant decrease in dG-C8-PhIP formation in LNCaP cells (Supplementary Figure 2B). However, the diminution in DNA binding seems to be due to a direct reaction of PABA and SMZ with *N*-acetoxy-PhIP, since both compounds alone strongly reduced the binding of synthetic *N*-acetoxy-PhIP to CT-DNA (Supplementary Figure 2A).

DNA binding studies with cytosolic fractions of LNCaP cells revealed that bioactivation of HONH-PhIP was mainly carried out by NATs, while the contributions of SULTs and kinases were relatively minor. In contrast, Nelson et al. reported that kinases were the most active Phase II enzymes in catalyzing HONH-PhIP binding to DNA (Nelson, *et al.*, 2001). However, that study employed a 200-fold higher concentration of HONH-PhIP compared to our conditions. These contrasting data suggest that the K_m values for the phosphorylation of HONH-PhIP are high for the kinases. Most cytosolic assays with Phase II enzyme bioactivation of HONH-HAAs employed high concentrations of substrate (up to 100 μM), which may have resulted in the appearance of enzyme activities that do not normally occur under realistic levels of human exposure to HAAs. We have shown that bioactivation of HONH-PhIP is predominantly catalyzed by NATs in human prostate cytosols. These data are in agreement with the LNCaP data and with a previous report on human prostate specimens (Di Paolo *et al.*, 2005). The authors detected N-acetylation of PABA and SMZ in human prostate cytosol; the levels of NAT1 activity were up to 100-fold higher than NAT2 activity. We detected similar rates of PABA N-acetylation; however, we did not detect NAT2 activity (Table 1). We also detected SULT1A1 activity in human prostate tissues, based on the sulfation of 4-nitrophenol (Table 1); previous studies only reported levels of SULT1A1 mRNA and protein expression (Al-Buheissi *et al.*, 2006; Martin, *et al.*, 2010).

We confirmed that the bioactivation of HONH-PhIP is carried out by recombinant NAT1 and NAT2, and the rates of NAT2 bioactivation, measured by dG-C8-PhIP adduct formation, were ~35-fold higher than for NAT1 (Supplementary Figure 3). These findings are consistent with previous studies (Hein *et al.*, 1994; Minchin *et al.*, 1992). However, the bioactivation of HOHN-PhIP, by NAT2, is relatively minor in bacterial or mammalian cells genetically engineered to express NAT2. In contrast, HONH-IQ, HONH-MeIQx, and HONH-AαC are efficiently bioactivated by NAT2 in these cells (Turesky and Le Marchand, 2011). Taken together, these findings suggest the plausible involvement of NAT1 in the bioactivation of HONH-PHIP in human prostate, particularly, in the absence of measurable NAT2 activity. Nevertheless, our inability to detect NAT2 activity, based on the N-acetylation of SMZ, does not rule out a potential contribution of residual NAT2 activity in the bioactivation of HONH-PhIP, as was previously suggested for human mammary tissue (Williams *et al.*, 2001). Indeed, the weak correlation between NAT1 activity and dG-C8-PhIP adduct formation in cytosolic assays suggests that low levels of NAT2 expressed in prostate or mammary tissue could contribute to dG-C8-PhIP adduct formation.

NATs are polymorphic enzymes, and several genotypes/phenotypes are classified as rapid, intermediate, or slow acetylators (Hein, 2009). In rats, the levels of dG-C8-PhIP formed in the prostate are higher in rapid NAT2 (orthologue of human NAT1) compared to slow NAT2 (Purewal *et al.*, 2000). In humans, several studies have examined the association between NATs genotypes and PC risk but provided inconsistent results. However, in 1 pilot study, an association of the putative rapid NAT1 acetylator (*NAT1*10*) combined with slow *NAT2* acetylator genotypes was reported to increase the susceptibility of PC over other combinations of NATs genotypes, an increase in PC risk (Hein *et al.*, 2002). It would be important to determine whether *NAT1*10* leads to a higher bioactivation of HONH-PhIP than other *NAT1* genotypes.

Overall, our findings show that HONH-PhIP is a potent DNA-damaging agent in the human prostate LNCaP cell line. The far greater susceptibility of this cell line to HONH-PhIP compared to other HONH-HAAs is consistent with rodent studies, where high levels of dG-C8-PhIP are formed in prostate and induce PC. Our emerging biomarker data show that PhIP, but not other prominent HAAs present in cooked meats, forms DNA adducts in human prostate. Further studies are required to better characterize the roles of Phase II enzymes and their genetic polymorphisms in the bioactivation of PhIP and PC risk.

SUPPLEMENTARY DATA

Supplementary data are available at *Toxicological Sciences* online.

ACKNOWLEDGMENTS

We thank Dr Badrinath Konety, MD, Department of Urology, University of Minnesota, for his interest and support of this project; Drew Sciacca, Department of Laboratory Medicine and Pathology, who handled the prostatectomy specimens and dissected appropriate tissue; and Beth Fenske, Dr Cole Drifka and the staff from BioNet Tissue Procurement, for collection of the prostate biospecimens.

FUNDING

National Cancer Institute of the National Institutes of Health (R01CA122320 to R.J.T.); National Center for Advancing Translational Sciences (NIH Award Number UL1TR000114). Mass spectrometry was carried out in the Analytical Biochemistry Shared Resource of the Masonic Cancer Center, University of Minnesota, funded in part by Cancer Center Support (CA-077598).

REFERENCES

Agus, C., Ilett, K. F., Kadlubar, F. F., and Minchin, R. F. (2000). Characterization of an ATP-dependent pathway of activation for the heterocyclic amine carcinogen N-hydroxy-2-amino-3-methylimidazo[4,5-f]quinoline. *Carcinogenesis* **21**, 1213–1219.

Al-Buheissi, S. Z., Patel, H. R., Meinl, W., Hewer, A., Bryan, R. L., Glatt, H., Miller, R. A., and Phillips, D. H. (2006). N-Acetyltransferase and sulfotransferase activity in human prostate: Potential for carcinogen activation. *Pharmacogenet. Genomics* **16**, 391–399.

Bessette, E. E., Yasa, I., Dunbar, D., Wilkens, L. R., Le Marchand, L., and Turesky, R. J. (2009). Biomonitoring of carcinogenic heterocyclic aromatic amines in hair: A validation study. *Chem. Res. Toxicol.* **22**, 1454–1463.

Bogen, K. T., Keating, G. A., 2nd, Chan, J. M., Paine, L. J., Simms, E. L., Nelson, D. O., and Holly, E. A. (2007). Highly elevated PSA and dietary PhIP intake in a prospective clinic-based study among African Americans. *Prostate. Cancer. Prostatic. Dis.* **10**, 261–269.

Borowsky, A. D., Dingley, K. H., Ubick, E., Turteltaub, K. W., Cardiff, R. D., and Devere-White, R. (2006). Inflammation and atrophy precede prostatic neoplasia in a PhIP-induced rat model. *Neoplasia* **8**, 708–715.

Bostwick, D. G., Burke, H. B., Djakiew, D., Euling, S., Ho, S. M., Landolph, J., Morrison, H., Sonawane, B., Shifflett, T., and Waters, D. J. (2004). Human prostate cancer risk factors. *Cancer* **101**, 2371–2490.

Bouvard, V., Loomis, D., Guyton, K. Z., Grosse, Y., Ghissassi, F. E., Benbrahim-Tallaa, L., Guha, N., Mattock, H., and Straif, K.; International Agency for Research on Cancer Monograph Working Group (2015). Carcinogenicity of consumption of red and processed meat. *Lancet Oncol.* **16**, 1599–1600.

Bradford, M. M. (1976). A rapid and sensitive method for the quantitation of microgram quantities of protein utilizing the principle of protein-dye binding. *Anal. Biochem.* **72**, 248–254.

Burke, M. D., and Mayer, R. T. (1983). Differential effects of phenobarbitone and 3-methylcholanthrene induction on the hepatic microsomal metabolism and cytochrome P-450-binding of phenoxazone and a homologous series of its n-alkyl ethers (alkoxyresorufins). *Chem. Biol. Interact.* **45**, 243–258.

Cai, T., Bellamri, M., Ming, X., Koh, W. P., Yu, M. C., and Turesky, R. J. (2017). Quantification of hemoglobin and white blood cell DNA adducts of the tobacco carcinogens 2-amino-9H-pyrido[2,3-b]indole and 4-aminobiphenyl formed in humans by nanoflow liquid chromatography/ion trap multistage mass spectrometry. *Chem. Res. Toxicol.* **30**, 1333–1343.

Chevereau, M., Glatt, H., Zalko, D., Cravedi, J. P., and Audebert, M. (2017). Role of human sulfotransferase 1A1 and N-acetyltransferase 2 in the metabolic activation of 16 heterocyclic amines and related heterocyclics to genotoxicants in recombinant V79 cells. *Arch. Toxicol.* **91**, 3175–3184.

Crow, P., Barrass, B., Kendall, C., Hart-Prieto, M., Wright, M., Persad, R., and Stone, N. (2005). The use of Raman spectroscopy to differentiate between different prostatic adenocarcinoma cell lines. *Br. J. Cancer* **92**, 2166–2170.

Di Paolo, O. A., Teitel, C. H., Nowell, S., Coles, B. F., and Kadlubar, F. F. (2005). Expression of cytochromes P450 and glutathione S-transferases in human prostate, and the potential for activation of heterocyclic amine carcinogens via acetyl-coA-, PAPS- and ATP-dependent pathways. *Int. J. Cancer* **117**, 8–13.

Donato, M. T., Montero, S., Castell, J. V., Gomez-Lechon, M. J., and Lahoz, A. (2010). Validated assay for studying activity profiles of human liver UGTs after drug exposure: Inhibition and induction studies. *Anal. Bioanal. Chem.* **396**, 2251–2263.

Dubey, V., and Owusu-Apenten, R. K. (2014). Curcumin restores glutathione-S-transferase activity for LNCaP prostate cancer cells. *Pure Appl. Chem.* **2**, 61–72.

Eugster, H. P., Probst, M., Wurgler, F. E., and Sengstag, C. (1993). Caffeine, estradiol, and progesterone interact with human CYP1A1 and CYP1A2. Evidence from cDNA-directed expression in *Saccharomyces cerevisiae*. *Drug Metab. Dispos.* **21**, 43–49.

Felton, J. S., Jagerstad, M., Knize, M. G., Skog, K., and Wakabayashi, K. (2000). Contents in foods, beverages and tobacco. In *Food Borne. Carcinogens Heterocyclic Amines* (M. Nagao and T. Sugimura, Eds.), pp. 31–71. John Wiley & Sons Ltd., Chichester, England.

Gann, P. H. (2002). Risk factors for prostate cancer. *Rev. Urol.* **4(Suppl 5)**, S3–S10.

Goodenough, A. K., Schut, H. A., and Turesky, R. J. (2007). Novel LC-ESI/MS/MS(n) method for the characterization and quantification of 2'-deoxyguanosine adducts of the dietary carcinogen 2-amino-1-methyl-6-phenylimidazo[4,5-b]pyridine by 2-D linear quadrupole ion trap mass spectrometry. *Chem. Res. Toxicol.* **20**, 263–276.

Grant, D. M., Blum, M., Beer, M., and Meyer, U. A. (1991). Monomorphic and polymorphic human arylamine N-acetyltransferases: A comparison of liver isozymes and expressed products of two cloned genes. *Mol. Pharmacol.* **39**, 184–191.

Hein, D. W. (2009). N-acetyltransferase SNPs: Emerging concepts serve as a paradigm for understanding complexities of personalized medicine. *Expert Opin. Drug Metab. Toxicol.* **5**, 353–366.

Hein, D. W., Leff, M. A., Ishibe, N., Sinha, R., Frazier, H. A., Doll, M. A., Xiao, G. H., Weinrich, M. C., and Caporaso, N. E. (2002). Association of prostate cancer with rapid N-acetyltransferase 1 (NAT1*10) in combination with slow N-acetyltransferase 2 acetylator genotypes in a pilot case-control study. *Environ. Mol. Mutagen.* **40**, 161–167.

Hein, D. W., Rustan, T. D., Ferguson, R. J., Doll, M. A., and Gray, K. (1994). Metabolic activation of aromatic and heterocyclic N-hydroxyarylamines by wild-type and mutant recombinant human NAT1 and NAT2 acetyltransferases. *Arch. Toxicol.* **68**, 129–133.

Hruba, E., Trilecova, L., Marvanova, S., Krcmar, P., Vykopalova, L., Milcova, A., Libalova, H., Topinka, J., Starsichova, A., Soucek, K., *et al.* (2010). Genotoxic polycyclic aromatic hydrocarbons fail to induce the p53-dependent DNA damage response, apoptosis or cell-cycle arrest in human prostate carcinoma LNCaP cells. *Toxicol. Lett.* **197**, 227–235.

International Agency for Research on Cancer (1993). Some naturally occurring substances: Food items and constituents, heterocyclic aromatic amines and mycotoxins. *IARC Monogr. Eval Carcinog. Risks Hum.* **56**, 1–599.

John, K., Ragavan, N., Pratt, M. M., Singh, P. B., Al-Buheissi, S., Matanhelia, S. S., Phillips, D. H., Poirier, M. C., and Martin, F. L. (2009). Quantification of phase I/II metabolizing enzyme gene expression and polycyclic aromatic hydrocarbon-DNA adduct levels in human prostate. *Prostate* **69**, 505–519.

King, R. S., Teitel, C. H., Shaddock, J. G., Casciano, D. A., and Kadlubar, F. F. (1999). Detoxification of carcinogenic aromatic and heterocyclic amines by enzymatic reduction of the N-hydroxy derivative. *Cancer Lett.* **143**, 167–171.

Kizu, R., Okamura, K., Toriba, A., Kakishima, H., Mizokami, A., Burnstein, K. L., and Hayakawa, K. (2003). A role of aryl hydrocarbon receptor in the antiandrogenic effects of polycyclic

aromatic hydrocarbons in LNCaP human prostate carcinoma cells. *Arch. Toxicol.* **77**, 335–343.

Knize, M. G., and Felton, J. S. (2005). Formation and human risk of carcinogenic heterocyclic amines formed from natural precursors in meat. *Nutr. Rev.* **63**, 158–165.

Li, G., Wang, H., Liu, A. B., Cheung, C., Reuhl, K. R., Bosland, M. C., and Yang, C. S. (2012). Dietary carcinogen 2-amino-1-methyl-6-phenylimidazo[4,5-b]pyridine-induced prostate carcinogenesis in CYP1A-humanized mice. *Cancer Prev. Res.* **5**, 963–972.

Mandair, D., Rossi, R. E., Pericleous, M., Whyand, T., and Caplin, M. E. (2014). Prostate cancer and the influence of dietary factors and supplements: A systematic review. *Nutr. Metab. (Lond)* **11**, 30.

Martin, F. L., Patel, I. I., Sozeri, O., Singh, P. B., Ragavan, N., Nicholson, C. M., Frei, E., Meinl, W., Glatt, H., Phillips, D. H., *et al.* (2010). Constitutive expression of bioactivating enzymes in normal human prostate suggests a capability to activate pro-carcinogens to DNA-damaging metabolites. *Prostate* **70**, 1586–1599.

McGuire, S. (2016). World Cancer Report 2014. Geneva, Switzerland: World Health Organization, International Agency for Research on Cancer, WHO Press, 2015. *Adv. Nutr.* **7**, 418–419.

Meerman, J. H., van Doorn, A. B., and Mulder, G. J. (1980). Inhibition of sulfate conjugation of N-hydroxy-2-acetylaminofluorene in isolated perfused rat liver and in the rat in vivo by pentachlorophenol and low sulfate. *Cancer Res.* **40**, 3772–3779.

Minchin, R. F., Reeves, P. T., Teitel, C. H., McManus, M. E., Mojarrabi, B., Ilett, K. F., and Kadlubar, F. F. (1992). N-and O-acetylation of aromatic and heterocyclic amine carcinogens by human monomorphic and polymorphic acetyltransferases expressed in COS-1 cells. *Biochem. Biophys. Res. Commun.* **185**, 839–844.

Muckel, E., Frandsen, H., and Glatt, H. R. (2002). Heterologous expression of human N-acetyltransferases 1 and 2 and sulfotransferase 1A1 in *Salmonella typhimurium* for mutagenicity testing of heterocyclic amines. *Food Chem. Toxicol.* **40**, 1063–1068.

Nakai, Y., Nelson, W. G., and De Marzo, A. M. (2007). The dietary charred meat carcinogen 2-amino-1-methyl-6-phenylimidazo[4, 5-b]pyridine acts as both a tumor initiator and promoter in the rat ventral prostate. *Cancer Res.* **67**, 1378–1384.

Nakai, Y., and Nonomura, N. (2013). Inflammation and prostate carcinogenesis. *Int. J. Urol.* **20**, 150–160.

Nauwelaers, G., Bessette, E. E., Gu, D., Tang, Y., Rageul, J., Fessard, V., Yuan, J.-M., Yu, M. C., Langouët, S., and Turesky, R. J. (2011). DNA adduct formation of 4-aminobiphenyl and heterocyclic aromatic amines in human hepatocytes. *Chem. Res. Toxicol.* **24**, 913–925.

Nelson, C. P., Kidd, L. C., Sauvageot, J., Isaacs, W. B., De Marzo, A. M., Groopman, J. D., Nelson, W. G., and Kensler, T. W. (2001). Protection against 2-hydroxyamino-1-methyl-6-phenylimidazo[4,5-b]pyridine cytotoxicity and DNA adduct formation in human prostate by glutathione S-transferase P1. *Cancer Res.* **61**, 103–109.

Oliveira, D. S., Dzinic, S., Bonfil, A. I., Saliganan, A. D., Sheng, S., and Bonfil, R. D. (2016). The mouse prostate: A basic anatomical and histological guideline. *Bosn. J. Basic Med. Sci.* **16**, 8–13.

Pathak, K. V., Bellamri, M., Wang, Y., Langouet, S., and Turesky, R. J. (2015). 2-Amino-9H-pyrido[2,3-b]indole (AalphaC) adducts and thiol oxidation of serum albumin as potential biomarkers of tobacco smoke. *J. Biol. Chem.* **290**, 16304–16318.

Purewal, M., Fretland, A. J., Schut, H. A., Hein, D. W., and Wargovich, M. J. (2000). Association between acetylator genotype and 2-amino-1-methyl-6-phenylimidazo[4,5-b]pyridine (PhIP) DNA adduct formation in colon and prostate of inbred Fischer 344 and Wistar Kyoto rats. *Cancer Lett.* **149**, 53–60.

Russell, A. J., Westwood, I. M., Crawford, M. H., Robinson, J., Kawamura, A., Redfield, C., Laurieri, N., Lowe, E. D., Davies, S. G., and Sim, E. (2009). Selective small molecule inhibitors of the potential breast cancer marker, human arylamine N-acetyltransferase 1, and its murine homologue, mouse arylamine N-acetyltransferase 2. *Bioorg. Med. Chem.* **17**, 905–918.

Shirai, T., Sano, M., Tamano, S., Takahashi, S., Hirose, M., Futakuchi, M., Hasegawa, R., Imaida, K., Matsumoto, K., and Wakabayashi, K. (1997). The prostate: A target for carcinogenicity of 2-amino-1-methyl-6-phenylimidazo[4,5-b]pyridine (PhIP) derived from cooked foods. *Cancer Res.* **57**, 195–198.

Siegel, R. L., Miller, K. D., and Jemal, A. (2016). Cancer statistics, 2016. *CA Cancer J. Clin.* **66**, 7–30.

Stuart, G. R., Holcroft, J., de Boer, J. G., and Glickman, B. W. (2000). Prostate mutations in rats induced by the suspected human carcinogen 2-amino-1-methyl-6-phenylimidazo[4,5-b]pyridine. *Cancer Res.* **60**, 266–268.

Sugimura, T., Wakabayashi, K., Nakagama, H., and Nagao, M. (2004). Heterocyclic amines: Mutagens/carcinogens produced during cooking of meat and fish. *Cancer Sci.* **95**, 290–299.

Tabrett, C. A., and Coughtrie, M. W. (2003). Phenol sulfotransferase 1A1 activity in human liver: Kinetic properties, interindividual variation and re-evaluation of the suitability of 4-nitrophenol as a probe substrate. *Biochem. Pharmacol.* **66**, 2089–2097.

Takayama, K., Kaneshiro, K., Tsutsumi, S., Horie-Inoue, K., Ikeda, K., Urano, T., Ijichi, N., Ouchi, Y., Shirahige, K., Aburatani, H., *et al.* (2007). Identification of novel androgen response genes in prostate cancer cells by coupling chromatin immunoprecipitation and genomic microarray analysis. *Oncogene* **26**, 4453–4463.

Tiang, J. M., Butcher, N. J., and Minchin, R. F. (2010). Small molecule inhibition of arylamine N-acetyltransferase Type I inhibits proliferation and invasiveness of MDA-MB-231 breast cancer cells. *Biochem. Biophys. Res. Commun.* **393**, 95–100.

Turesky, R. J., Konorev, D., Fan, X., Tang, Y., Yao, L., Ding, X., Xie, F., Zhu, Y., and Zhang, Q. Y. (2015). Effect of cytochrome P450 reductase deficiency on 2-amino-9H-pyrido[2,3-b]indole metabolism and DNA adduct formation in liver and extrahepatic tissues of mice. *Chem. Res. Toxicol.* **28**, 2400–2410.

Turesky, R. J., Lang, N. P., Butler, M. A., Teitel, C. H., and Kadlubar, F. F. (1991). Metabolic activation of carcinogenic heterocyclic aromatic amines by human liver and colon. *Carcinogenesis* **12**, 1839–1845.

Turesky, R. J., and Le Marchand, L. (2011). Metabolism and biomarkers of heterocyclic aromatic amines in molecular epidemiology studies: Lessons learned from aromatic amines. *Chem. Res. Toxicol.* **24**, 1169–1214.

Vietri, M., De Santi, C., Pietrabissa, A., Mosca, F., and Pacifici, G. M. (2000). Inhibition of human liver phenol sulfotransferase by nonsteroidal anti-inflammatory drugs. *Eur. J. Clin. Pharmacol.* **56**, 81–87.

Wang, C. Y., Debiec-Rychter, M., Schut, H. A., Morse, P., Jones, R. F., Archer, C., King, C. M., and Haas, G. P. (1999). N-Acetyltransferase expression and DNA binding of N-hydroxyheterocyclic amines in human prostate epithelium. *Carcinogenesis* **20**, 1591–1595.

Wang, Y., Peng, L., Bellamri, M., Langouet, S., and Turesky, R. J. (2015). Mass spectrometric characterization of human serum albumin adducts formed with N-oxidized metabolites of 2-amino-1-methylphenylimidazo[4,5-b]pyridine in human plasma and hepatocytes. *Chem. Res. Toxicol.* **28**, 1045–1059.

Williams, J. A., Stone, E. M., Fakis, G., Johnson, N., Cordell, J. A., Meinl, W., Glatt, H., Sim, E., and Phillips, D. H. (2001). N-Acetyltransferases, sulfotransferases and heterocyclic amine activation in the breast. *Pharmacogenetics* **11**, 373–388.

Xiao, S., Guo, J., Yun, B. H., Villalta, P. W., Krishna, S., Tejpaul, R., Murugan, P., Weight, C. J., and Turesky, R. J. (2016). Biomonitoring DNA adducts of cooked meat carcinogens in human prostate by nano liquid chromatography-high resolution tandem mass spectrometry: Identification of 2-amino-1-methyl-6-phenylimidazo[4,5-b]pyridine DNA adduct. *Anal. Chem.* **88**, 12508–12515.